Cowpox virus encodes a protein that binds B7.1 and B7.2 and subverts T cell costimulation

Xiaoli Wang[a,1], Sytse J. Piersma[b,1], Jabari I. Elliott[a], John M. Errico[a], Maria D. Gainey[b,2], Liping Yang[b], Christopher A. Nelson[a], Wayne M. Yokoyama[a,b,3], and Daved H. Fremont[a,c,d,3]

[a]Department of Pathology and Immunology, Washington University School of Medicine in St. Louis, St. Louis, MO 63110; [b]Division of Rheumatology, Department of Medicine, Washington University School of Medicine in St. Louis, St. Louis, MO 63110; [c]Department of Biochemistry and Molecular Biophysics, Washington University School of Medicine in St. Louis, St. Louis, MO 63110; and [d]Department of Molecular Microbiology, Washington University School of Medicine in St. Louis, St. Louis, MO 63110

Contributed by Wayne M. Yokoyama, August 26, 2019 (sent for review May 31, 2019; reviewed by Stuart N. Isaacs and Marc K. Jenkins)

Costimulation is required for optimal T cell activation, yet it is unclear whether poxviruses dedicatedly subvert costimulation during infection. Here, we report that the secreted M2 protein encoded by cowpox virus (CPXV) specifically interacts with human and murine B7.1 (CD80) and B7.2 (CD86). We also show that M2 competes with CD28 and CTLA4 for binding to cell surface B7 ligands, with stronger efficacy against CD28. Functionally, recombinant M2 and culture supernatants from wild-type (WT) but not M2-deficient (ΔM2) CPXV-infected cells can potently suppress B7 ligand-mediated T cell proliferation and interleukin-2 (IL-2) production. Furthermore, we observed increased antiviral CD4 and CD8 T cell responses in C57BL/6 mice challenged by ΔM2 CPXV compared with WT virus. These differences in immune responses to ΔM2 and WT CPXV were not observed in CD28-deficient mice. Taken together, our findings define a mechanism of viral sabotage of T cell activation that highlights the role of CD28 costimulation in host defense against poxvirus infections.

cowpox virus | immune evasion | T cell

Orthopoxviruses are a genus of large double-stranded DNA viruses that includes the causative agent of smallpox, variola virus. Smallpox was declared eradicated in 1980 upon successful worldwide vaccination using attenuated vaccinia virus (VACV). However, since the cessation of vaccinations, 2 related zoonotic orthopoxviruses, cowpox virus (CPXV) and monkeypox virus (MPXV), have emerged with sporadic human outbreaks (1). Unlike MPXV infection, which can develop smallpox-like symptoms, human CPXV infection in healthy individuals usually only causes localized skin lesions; however, in immunocompromised patients, the infection may lead to severe and even lethal outcomes (2, 3). Among the orthopoxviruses, CPXV has the largest genome and has been considered the ancestor of all of the modern orthopoxviruses. Moreover, CPXV is endemic in rodents and can readily infect laboratory mice.

Orthopoxviruses dedicate a significant fraction of their genome to undermining host immune defenses. Of particular interest is the poxvirus immune evasion (PIE) domain-containing family of proteins, which are typically dispensable for viral entry and replication (4). Members of the PIE family all contain signal peptides for targeting to the secretory pathway and are predicted to adopt a conserved β-sandwich fold that is unique to poxvirus-encoded proteins. Diverse functions have been ascribed to PIE proteins, including the sequestration of proinflammatory chemokines and helical bundle cytokines. We and others previously found that a CPXV-encoded PIE protein, CPXV203, sabotages major histocompatibility complex (MHC) class I antigen presentation, thereby preventing CD8 T cell recognition of infected cells and increasing morbidity in laboratory mice (5–7).

T cell responses are essential in adaptive immunity to viral infection. Optimal T cell activation is characterized by rapid proliferation, cytokine production, and efficient effector function, which, in addition to T cell receptor engagement, requires engagement of costimulatory receptors with their ligands that are expressed mainly by antigen-presenting cells (APCs) (8). The CD28 receptor, and its ligands B7.2 (CD86) and B7.1 (CD80), was the first costimulatory pathway identified and plays a central role in facilitating T cell activation (9). A related receptor, CTLA4, also binds B7.1 and B7.2, but engagement negatively regulates T cell activation, thereby antagonizing CD28 function (10). Blockade of CTLA4 is now used in the clinic as part of cancer immunotherapy (11). Regulation of CD28 and CTLA4 interaction with their ligands is critical for T cell homeostasis and maintenance of peripheral tolerance, yet the role of costimulation in the host response to viral infection has not been well resolved (12, 13). Nevertheless, the CD28 pathway is targeted by some herpesviruses. For example, Kaposi's sarcoma-associated herpesvirus encodes a ubiquitin ligase, kK5, that induces degradation of B7.2 along with other host immune modulators (14, 15). Murine cytomegalovirus (MCMV) encodes 2 proteins that are associated with B7.1 and B7.2 down-regulation, and similar down-regulation was also observed in human cytomegalovirus-infected dendritic cells (DCs) (16–19). Further, mice lacking both B7.1 and B7.2 showed reduced early expansion of MCMV-specific CD4 T cells, whereas an MCMV mutant lacking m138 and m147.5 open reading frames (ORFs) induced a more robust CD4 T cell response (20). While the role of costimulation has not been explored in CPXV infections,

Significance

After eradication of smallpox, zoonotic orthopoxviruses, including cowpox virus (CPXV) and monkeypox virus, continue to be a source for infection in humans. Poxviruses dedicate a significant part of their genome encoding proteins that effectively undermine host immune defenses. Here, we demonstrate that a CPXV-encoded protein, M2, can specifically bind B7.1 (CD80) and B7.2 (CD86), cell surface proteins expressed mainly by professional antigen-presenting cells that serve as ligands of the T cell costimulatory receptor CD28 and inhibitory receptor CTLA4. Functionally, we found that M2 blocks CD28-mediated T cell activation in vitro and in a mouse model of cowpox infection.

Author contributions: X.W., S.J.P., C.A.N., W.M.Y., and D.H.F. designed research; X.W., S.J.P., J.I.E., J.M.E., M.D.G., L.Y., and C.A.N. performed research; M.D.G., C.A.N., and W.M.Y. contributed new reagents/analytic tools; X.W., S.J.P., J.I.E., W.M.Y., and D.H.F. analyzed data; and X.W., S.J.P., W.M.Y., and D.H.F. wrote the paper.

Reviewers: S.N.I., University of Pennsylvania; and M.K.J., University of Minnesota.

The authors declare no conflict of interest.

[1]X.W. and S.J.P. contributed equally to this work.

[2]Present address: Department of Biology, Western Carolina University, Cullowhee, NC 28723.

[3]To whom correspondence may be addressed. Email: yokoyama@wustl.edu or fremont@wustl.edu.

This article contains supporting information online at www.pnas.org/lookup/suppl/doi:10.1073/pnas.1909414116/-/DCSupplemental.

First published October 1, 2019.

previous studies have revealed that T cell responses against the orthopoxviruses ectromelia and vaccinia are dependent, in part, on CD28 costimulation (21, 22).

Here, we report that the CPXV M2 protein specifically binds B7.1 and B7.2 but no other B7 family members. In the CPXV Brighton Red strain, M2 is encoded by ORF *CPXV040*, a PIE family protein named after a 95% similar protein encoded by the *M2L* ORF of the VACV Copenhagen strain (4, 23). We demonstrate that M2 competes with CD28 and CTLA4 for binding to human and murine B7.1 and B7.2; however, at lower concentrations, it primarily competes with CD28. Consistently, recombinant M2 or culture supernatants from wild-type (WT) but not M2-deficient (ΔM2) CPXV-infected cells can potently suppress B7.2-mediated T cell proliferation and interleukin-2 (IL-2) production. Furthermore, we observed increased antiviral CD4 and CD8 responses in C57BL/6 mice challenged by ΔM2 CPXV compared with WT CPXV. The differences in immune responses to ΔM2 and WT CPXV were no longer preserved in CD28-deficient mice. These data thus provide strong evidence for T cell response sabotage by M2 in a CD28-dependent manner in vivo. Collectively, our findings define a mechanism of immune evasion where T cell costimulation is blocked by a protein secreted by virally infected cells.

Results

Identification of B7.1 (CD80) and B7.2 (CD86) as Candidate Ligands of CPXV M2. CPXV encodes at least 10 PIE domain-containing proteins, many of unknown function (4). We set out to functionally examine one of these proteins, M2, that is generally conserved across poxvirus genomes, including variola, MPXV, and some vaccinia viruses, suggesting that it may target a commonly used, conserved immune function. To search for potential M2 ligands or receptors, we purified C-terminal 6His-tagged M2 from the supernatant of transfected human 293F cells, which established that M2 is a secreted protein capable of forming high-order oligomers (*SI Appendix*, Fig. S1). We then biotinylated purified M2 (bio-M2) and analyzed its binding capacity to various cell lines in a flow cytometry-based screen. Among the cell lines tested, bio-M2 appeared to bind primarily to professional APCs, including murine and human B cell lines and a murine DC line, but not fibroblasts (Fig. 1*A*). We chose the human B lymphoma cell line RPMI8866 that displayed strong bio-M2 binding for coprecipitation and tandem mass spectrometry (MS/MS) analysis. Another CPXV PIE protein, C8, that has a distinct binding profile to the examined cell lines, was used as a control. Two independent analyses were conducted, using either in gel digestion or in solution digestion of the precipitates (Fig. 1*B*). B7.1 and B7.2 were the top hits from both analyses and were the only 2 plasma membrane-associated proteins reproducibly observed (Fig. 1*B* and *SI Appendix*, Fig. S2 and Tables S1 and S2). Consistent with our flow cytometry screen, B7.2 and B7.1 are known to be expressed mainly on APCs but not by fibroblasts (8), which distinguishes them from the other identified cell membrane proteins. Thus, collectively, these analyses strongly suggest that B7.2 and B7.1 are candidate interacting partners of M2.

M2 Specifically Binds to B7.2 and B7.1 and Differentially Blocks Their Receptor Interactions. To verify M2 binding to B7.2 and B7.1, we transduced mouse embryonic fibroblasts (MEFs) to express mouse or human B7.2 (MEF-m/hB7.2) and B7.1 (MEF-m/hB7.1) (Fig. 2 *A*, *Upper*). Flow cytometric analyses with these transduced cells showed that bio-M2 stained MEFs expressing mouse and human B7.1 and B7.2 but not the parental MEFs (Fig. 2 *A*, *Lower*). A similar analysis was conducted to examine binding of M2 with the other B7 family members that share similar ectodomains with B7.1 and B7.2. We tested murine PD-L1 and PD-L2 and human B7-H2, B7-H3, B7-H4, and B7-H6 by ectopically expressing constructs in Chinese hamster ovary (CHO) or

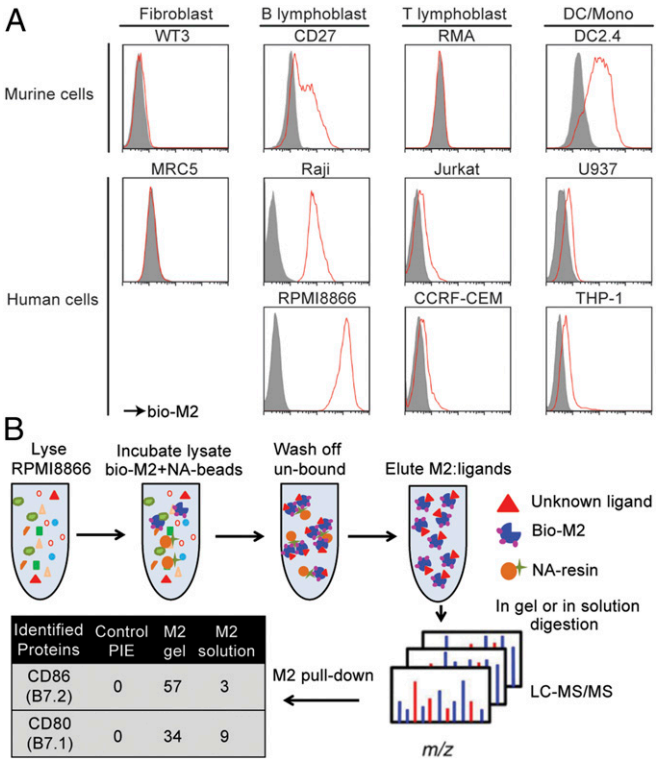

Fig. 1. Identification of B7.1 and B7.2 as candidate M2 ligands. (*A*) Cell lines were incubated with biotin-labeled CPXV^{BR} M2 (bio-M2) and stained by PE Streptavidin. Results representative of at least 2 independent flow cytometric analyses for each cell type are shown. (*B*) Pull-down MS approach to find M2 ligands. RPMI8866 cells were lysed in 1% Nonidet P-40, followed by incubation with 100 nM bio-M2 or bio-CPXV^{BR} C8 (PIE control) and NeutrAvidin (NA) resin for 2 h at 4 °C. Precipitates were separated by sodium dodecyl sulfate polyacrylamide gel electrophoresis, and gel bands were digested with trypsin. Alternatively, precipitates were digested in solution as described in *Materials and Methods*. Digested peptides were analyzed by LC-MS/MS. B7.1 and B7.2 were the only 2 cell membrane proteins reproducibly identified in M2 precipitations (*SI Appendix*, Fig. S2 and Tables S1 and S2).

293T cells and staining with bio-M2 (Fig. 2*B* and *SI Appendix*, Fig. S3). This analysis indicated that M2 specifically binds only B7.1 and B7.2 in the B7 family.

Human B7.1 and B7.2 are reported to organize differently on cell surfaces and exhibit different binding affinities to CD28 and CTLA4. Overall, hB7.1 shows higher affinity to the receptors than hB7.2, but both bind CTLA4 more tightly than they bind CD28 (24). Given this, we asked next whether M2 engages B7.1 and B7.2 similarly and whether it can comparably compete with CD28 or CTLA4 receptors. While preincubation of M2 with MEF-mB7.1/mB7.2 cells interfered with antibody recognition of mB7.2 in a dose-dependent manner, it had only a mild effect on staining by an anti-mB7.1 antibody, hinting that M2 may bind mB7.2 more tightly than mB7.1 (Fig. 3*A*). Although the epitopes of the antibodies are not known, they both can block receptor stimulation, suggesting that M2 may differentially block receptor engagement by B7.1 and B7.2. Indeed, in a dose-dependent manner, M2 competed efficiently with soluble mouse CD28-Fc and less efficiently with soluble mouse CTLA4-Fc for binding to mB7.2 on the surface of MEF cells. In comparison, at equal concentrations, M2 only moderately inhibited mouse CD28-Fc binding to mB7.1 and had no effect on mouse CTLA4-Fc binding to B7.1 (Fig. 3*B*). Taken together, these data indicate that M2 specifically binds mB7.2 and mB7.1 and primarily interferes with engagement of the stimulatory receptor CD28 with B7.2. We also examined the ability of M2 to disrupt human B7 proteins binding to human receptors, finding that hB7.1 and

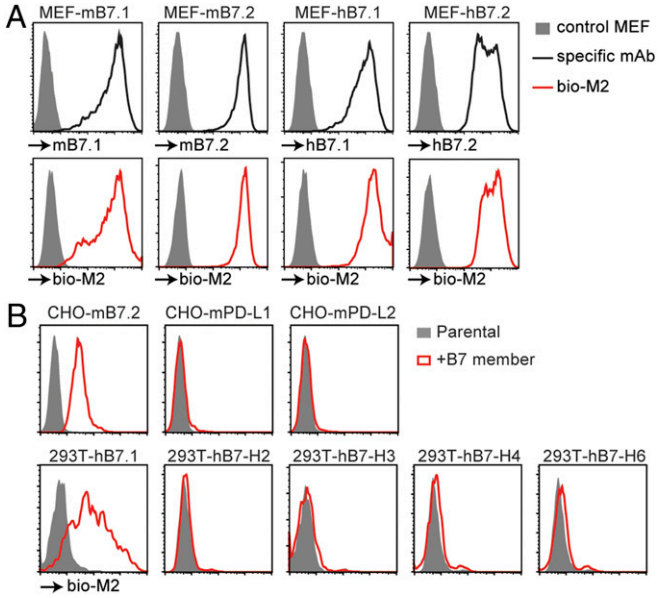

Fig. 2. M2 specifically binds B7.1 and B7.2. (*A*) MEFs transduced to stably express mouse or human B7.1 or B7.2 were verified by specific antibodies (*Upper*) and stained by bio-M2 followed by PE Streptavidin (*Lower*). mAb, monoclonal antibody. (*B*, *Upper*) Mouse PD-L1/2–transduced CHO cells were stained with bio-M2. CHO-mB7.2 cells served as a positive control. (*B*, *Lower*) 293T cells were transiently transfected to express the indicated human B7 family members. Flow cytometric analysis was conducted 48 h post-transfection. Ectopically expressed B7 family members were assessed by specific antibodies or cotransfected GFP (*SI Appendix*, Fig. S3).

hB7.2 engagement by human CD28-Fc is potently disrupted, while human CTLA4-Fc is blocked less efficiently (Fig. 3*C*).

Recent reports identified PD-L1 as a third ligand for B7.1 (25, 26). However, the interaction of the 2 proteins appears to occur *in cis* on the cell surface, where it may regulate optimal T cell responses (27, 28). Based on these reports and the critical role of PD-L1–mediated immunosuppression in regulation of peripheral tolerance, we also assessed the impact of M2 on the interaction of soluble PD-L1 with cell surface B7.1. As illustrated in Fig. 3*B*, MEF-mB7.1 or MEF-hB7.1 cells were incubated with soluble mouse or human PD-L1-Fc and different concentrations of M2. The binding of PD-L1-Fc was then evidenced with fluorescence-conjugated anti-Fc antibodies by flow cytometry. Surprisingly, we found that the presence of M2 could dramatically increase the binding of soluble hPD-L1-Fc to hB7.1-transduced cells. However, increased hPD-L1-Fc staining was M2 concentration-dependent, with the greatest augmentation observed in the presence of a medium concentration of M2. While we also observed increased mPD-L1-Fc staining of mB7.1-transduced cells, the increase was minor compared with the human proteins (*SI Appendix*, Fig. S4).

M2 Inhibits Ex Vivo T Cell Activation via Blockade of B7-Mediated Costimulation. To test the biological impact of M2 binding to B7 proteins, an ex vivo T cell activation assay was conducted. Splenic T cells from C57BL/6 mice were cocultured with MEF-mB7.2 cells in the presence of M2 or controls in plates coated with suboptimal anti-CD3ε. After 2 to 3 d, cell proliferation was determined by flow cytometric analysis and IL-2 production was measured by enzyme-linked immunosorbent assay (ELISA). Upon coculture with MEF-mB7.2, CD4 T cells significantly proliferated, as indicated by dilution of carboxyfluorescein succinimidyl ester (CFSE). The proliferation was mediated by expression of mB7.2 because it could be ablated by mB7.2 blocking antibody but not an immunoglobulin (Ig) control. Similar to blocking antibodies, addition of M2 in the culture resulted in significant inhibition of CD4 cell proliferation (Fig. 4*A*). Significant decreases in IL-2 production similar to the level of inhibition by anti-mB7.2 antibodies were also evidenced when splenic T cells were cocultured with MEF-mB7.2 in the presence of M2 (Fig. 4 *B*, *Right*). In comparison, splenic T cells cocultured with MEF-mB7.1 cells showed less efficient inhibition of IL-2 production by M2 (Fig. 4 *B*, *Left*). This is consistent with the stronger competition of M2 with soluble CD28 for binding to mB7.2 over mB7.1. Nevertheless, significant inhibition in IL-2 production mediated by M2 was observed when spleen cells were cocultured with a B cell line that endogenously expresses both B7.2 and B7.1 (*SI Appendix*, Fig. S5*A*). The level of inhibition by M2 in this setting is stronger than the antibody that only blocks B7.2 costimulation, suggesting M2 sabotages costimulation of T cells mediated by both B7.1 and B7.2, which results in an additive inhibitory effect (Fig. 4*C*). To further evaluate the physiological relevance of M2-mediated inhibition of T cell activation, we generated a bacterial artificial chromosome-derived WT or ORF*040*-deleted CPXV (WT or ΔM2 CPXV). Instead of using recombinant M2, we tested effects of the culture supernatants collected from Vero cells infected with WT or ΔM2 CPXV at a multiplicity of infection (MOI) of 0.5 or 1.0 in T cell and MEF-mB7.2 cocultures. A significant inhibitory effect in culture supernatant on IL-2 production was evidenced as early as 12 or 24 h postinfection with 1.0 MOI or 0.5 MOI of WT CPXV, respectively, but not with ΔM2 CPXV (Fig. 4*D* and *SI Appendix*,

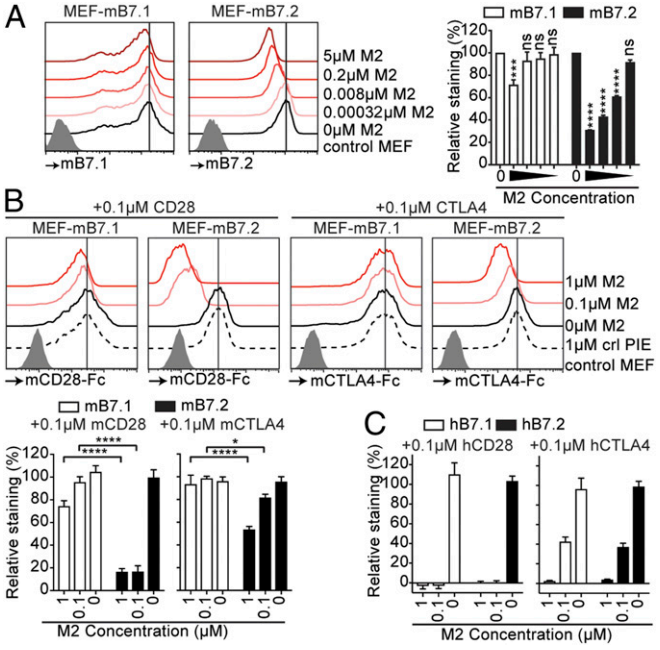

Fig. 3. M2 differentially blocks recognition of B7.1 and B7.2 by antibodies and the CD28 and CTLA4 receptors. (*A*, *Left*) MEFs transduced to express mouse B7.1 or B7.2 (MEF-mB7.1 or MEF-mB7.2) were preincubated with M2 at the indicated concentration before staining with 1 μg/mL anti-mouse B7.1 (16-10A1) or B7.2 (GL1) blocking antibody. (*A*, *Right*) Quantification of mean fluorescence intensity (MFI) of specific antibody staining in the presence of M2 relative to no M2 from 2 independent experiments is shown in the bar chart (mean ± SEM). ns, not significant. (*B*) Cells used in *A* were incubated with recombinant M2 or C8 (control PIE) and mouse CD28-Fc or CTLA4-Fc at the indicated concentration for 30 min before CD28-Fc/CTLA4-Fc binding was visualized by fluorescence-labeled anti-human IgG. (*Upper*) Representative flow cytometric plots of 3 independent analyses are shown. (*Lower*) Bar chart is the quantification of 3 analyses (mean ± SEM) showing MFI of CD28/CTLA4 in the presence of M2 relative to no M2. (*C*) Same experiment as in *B* was conducted with MEF-hB7.1 or MEF-hB7.2 and soluble human CD28-Fc or CTLA4-Fc. *$P < 0.05$, ***$P < 0.001$, ****$P < 0001$.

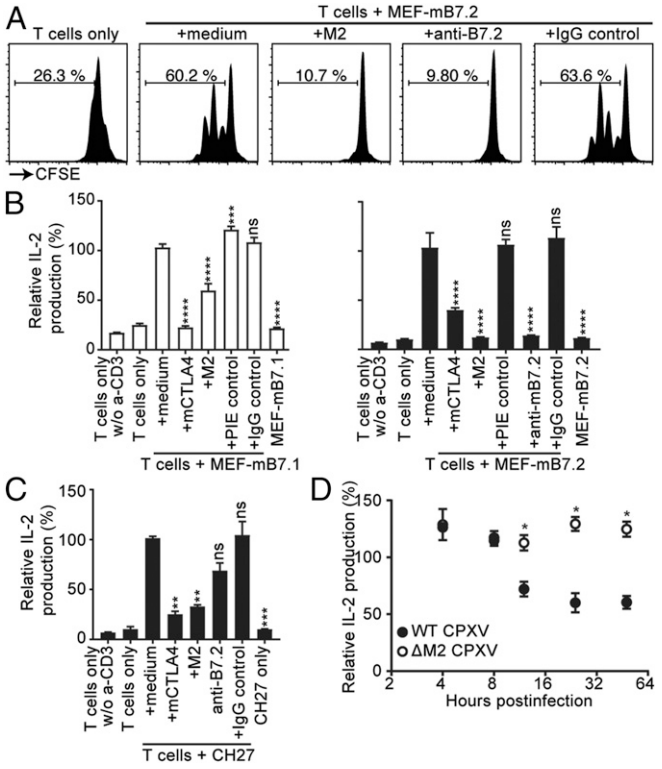

Fig. 4. M2 inhibits ex vivo T cell proliferation and activation costimulated by B7.1 and B7.2. (*A*) CFSE-labeled splenic T cells from C57BL/6 mice were stimulated for 3 d with MEF-mB7.2 cells in medium containing 400 nM M2, 1 μg/mL anti-mB7.2 (GL1), or IgG control in an anti-CD3ε–coated plate. CD4 cell proliferation was determined by CFSE dilution in the $CD3^+CD4^+$ population. (*B*) Enriched splenic T cells were cocultured with MEF-mB7.1/mB7.2 cells for 2 d in an anti-CD3ε (a-CD3)–coated plate. M2 and anti-mB7.2 antibodies were used as in *A*, irrelevant CPXV-PIE protein C8 and mouse CTLA4-Fc were used at 400 nM and 50 nM, respectively. The relative IL-2 production percentage in the presence of M2 or controls was calculated using splenic T cells + MEF only (+medium) as 100%. Results representative of 2 independent analyses are shown (triplicates, mean ± SD). ns, not significant; w/o, without. (*C*) CH27 cells were used as a stimulator in T cell activation as described in *B*. (*D*) Culture supernatants harvested at the indicated time from Vero cells infected with WT or ΔM2 CPXV (MOI = 1) were used in a T cell activation assay. Findings representative of 2 experiments (triplicates, mean ± SD) are shown. $^{**}P < 0.01$, $^{***}P < 0.001$, $^{****}P < 0001$.

Fig. S5*B*). A comparable inhibitory effect was seen with recombinant M2 at nanomolar concentrations (*SI Appendix*, Fig. S5*C*). These data clearly demonstrate that functional M2, encoded by the ORF*040* of CPXV, is secreted by infected cells and is sufficient to inhibit T cell activation mediated by B7.2 and CD3, thus providing strong evidence for an adaptive immune evasion function of the viral protein.

M2 Undermines CD4 and CD8 T Cell Responses during CPXV Infection In Vivo. To determine the contribution of M2 in subverting T cell responses during viral infection in vivo, C57BL/6 mice were intraperitoneally infected with ΔM2 or WT CPXV. Infection with ΔM2 CPXV elicited approximately a 2-fold stronger B8R-specific CD8 T cell response than WT CPXV as determined by enumeration of B8R tetramer-positive CD8 T cells in the spleen of infected C57BL/6 mice (Fig. 5*A*). Further analysis revealed a similar effect on interferon-γ (IFN-γ) production by bulk CPXV-specific CD8 T cells upon restimulation ex vivo with Δ12Δ203 CPXV-infected DC2.4 cells (Fig. 5*B*). The CPXV-specific CD4 T cell response was examined using DC2.4 cells loaded with a peptide pool of known VACV CD4 T cell epitopes that cross-reacted with CPXV (*SI Appendix*, Fig. S6). We observed an ∼2-fold increase in the percentage of IFN-γ–positive CD4 T cells in mice infected with ΔM2 CPXV compared with WT CPXV upon restimulation of splenocytes ex vivo (Fig. 5*C*). The increased T cell responses were not caused by increased antigen load as the ΔM2 CPXV titers were slightly lower, albeit not significant, than WT CPXV titers (Fig. 5*D*). B7-mediated costimulation is essential for mounting a CPXV-specific T cell response, as CD28-deficient animals failed to generate a CPXV-specific T cell response (Fig. 5*E*). Of note, mice infected with WT CPXV mounted a higher CD4 T cell response in C57BL/6 mice than in CD28-deficient animals, suggesting that M2 did not completely block CD28-mediated costimulation under the conditions tested. The in vivo data indicate that during CPXV infection, M2 can interfere with the expansion of CPXV-specific CD4 and CD8 T cell responses via binding B7 proteins and disrupting their role in costimulation.

Discussion

We here report that the CPXV-encoded protein M2 is secreted during viral infection, capably binds human and murine B7.1 and B7.2, and sabotages T cell costimulation both in vitro and in vivo. We found that recombinant M2, as well as supernatant of CPXV-infected cells containing M2, could significantly hamper ex vivo T cell activation mediated by B7 ligands. As a secreted protein, M2 could act on uninfected APCs to block costimulation of CD4 and CD8 T cells, even at sites distant from infection. Indeed, we detected increased in vivo CD4 and CD8 T cell responses to CPXV upon deletion of the M2-encoding ORF. These findings thus provide strong evidence that M2 functions to disrupt host adaptive immune surveillance by selectively blocking CD28 costimulation in the context of poxvirus infection.

Although B7.1 and B7.2 share structural similarity and both interact with CD28 and CTLA4, they are not functionally

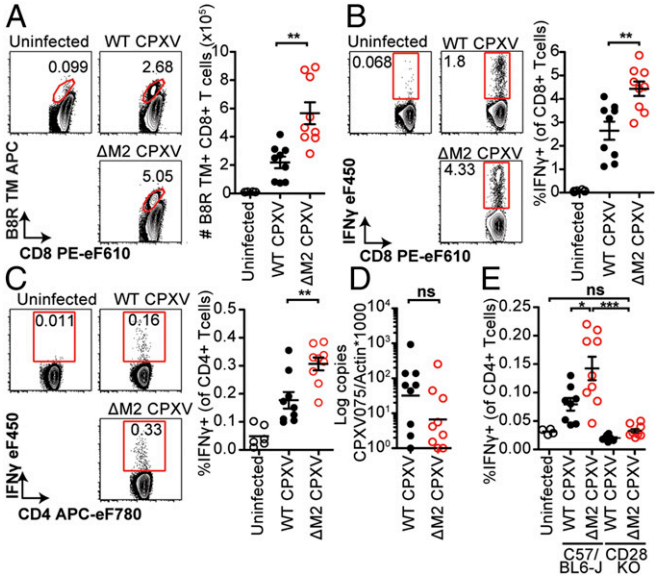

Fig. 5. ΔM2 CPXV elicits stronger primary T cell responses than WT CPXV. C57BL/6-CR mice were intraperitoneally infected with 50,000 platelet-forming units (PFU) of WT or ΔM2 CPXV. Spleens were analyzed 5 d postinfection. (*A*) B8R (peptide TSYKFESV) tetramer (TM) staining and total numbers (#) of tetramer-positive CD8 T cells. (*B*) Percentage of IFN-γ–producing CD8 T cells upon ex vivo stimulation with Δ12Δ203 CPXV-infected DC2.4 cells. (*C*) Percentage of IFN-γ–producing CD4 T cells upon ex vivo stimulation with peptide-pulsed DC2.4 cells. (*D*) CPXV titers in the spleen determined by DNA copy number. (*E*) C57BL/6-J WT and $CD28^{-/-}$ mice were intraperitoneally infected with 50,000 PFU of WT or ΔM2 CPXV and analyzed as in *C*. $^{*}P < 0.05$, $^{**}P < 0.01$, $^{***}P < 0.001$. ns. not significant.

redundant. Some animal in vivo studies indicate that B7.1 functions more as a negative modulator of immune responses, whereas B7.2 functions mostly as a stimulatory factor. For example, blockade of B7.1 in nonobese diabetic (NOD) mice severely exacerbates diabetes. In contrast, blockade of B7.2 prevents NOD mice from developing disease (29). The functional difference of the 2 ligands depends, at least in part, on differences in their expression kinetics, oligomeric status, and binding strength to CD28 and CTLA4. B7.2 is more abundant and up-regulated much earlier than B7.1 on APCs upon activation (30, 31) On the other hand, CD28 is expressed constitutively and broadly on naive T cells, whereas CTLA4 is normally only expressed on activated T cells upon costimulation by CD28 (32, 33). Moreover, biophysical studies indicate that although both CTLA4 and CD28 are expressed as homodimers, CTLA4 appears to uniquely bind ligands multivalently (24, 34). On the ligand side, B7.1 presents mostly as a homodimer, while B7.2 is thought to be monomeric (34–36). Collectively, these observations have been used to argue that while CTLA4 interacts preferentially with B7.1, B7.2 is likely the dominant ligand for CD28, especially at early stages of T cell activation.

In this study, we found that M2 preferentially blocks murine B7.2 interaction with CD28, but barely affects B7.1 receptor engagement despite capable binding to both B7 ligands. Consistent with the role of CD28 costimulation in T cell activation and proliferation, we found that M2 serves to limit the expansion of viral-specific CD4 and CD8 T cells in a mouse model of CPXV infection. Our experiments using human reagents indicate that M2 also preferentially disrupts CD28 ligand recognition, but in contrast to the mouse, M2 does not appear to discriminate between human B7.1 and B7.2. We also found that M2 might have the capacity to significantly modulate human PD-L1 interactions with B7.1, although further experiments will be needed to address the physiological significance of this observation, which is much less dramatic using murine proteins. Consistent with these M2 studies, we have previously reported that two other CPXV immune evasion proteins bind human targets with equal or higher affinity than the equivalent mouse proteins. For example, CPXV203 binds all human and murine MHC-I alleles, preventing them from trafficking to the cell surface (7), and CPXV OMCP serves as a soluble antagonist of NKG2D with a substantially higher affinity to the human receptor as compared to the mouse (37). Since rodents serve as a natural reservoir for CPXV while humans are only an accidental host, this phenomenon might be a consequence of pathogen–host coevolution in rodents but not in humans.

Advances in understanding of the pivotal role of B7-mediated costimulation in the regulation of self-tolerance have enabled strategies for the treatment of transplant rejection and autoimmune diseases (38, 39). For example, an engineered CTLA4-Ig fusion protein capable of binding B7.1 and B7.2 has proven efficacious in ameliorating symptoms of several autoimmune diseases (40). Although promising, this strategy suffers from the concern that nonselective blockade of CD28 versus CTLA4 signaling may contribute to adverse effects in certain circumstances (41). In this context, we speculate that once we better understand how M2 selectively disrupts CD28 costimulation, we may open up new avenues for the development of therapeutic agents for the treatment of autoimmune diseases or transplant rejection.

CPXV is unique among the orthopoxviruses in that it encodes 2 proteins, 12 and 203, that synergistically disable MHC class I presentation in infected cells (5–7). However, this immune evasion strategy does not affect T cell priming, which likely is driven by cross-presentation of viral antigen (42). We now show that CPXV can sabotage T cell activation and proliferation by a separate mechanism that targets T cell costimulation with the secreted M2 protein. Interestingly, *M2* or *M2-like* ORFs are found distributed among many poxvirus genomes that are not known to down-regulate MHC class I antigen presentation, including most orthopoxviruses, leporipoxviruses, yatapoxviruses, and cervidpoxviruses (4). Ectromelia virus does not appear to encode an M2 protein, and infections provoke a considerably stronger virus-specific CD4 T cell response in comparison to VACV-WR, which does have an M2 protein (43), consistent with our experiments with ΔM2 CPXV compared with WT CPXV. Various strains of VACV have been used as vaccines or vectors to treat a number of infections, as well as cancers (44, 45). A recent study reported that the M2 protein encoded by the VACV Copenhagen strain can also bind B7 ligands (46), and notably, M2 is absent from certain attenuated VACV strains, for example, modified vaccinia virus Ankara and its derivative Acam3000. Taken together, these findings have implications for the design of poxvirus-based vectors where deletion of the *M2* ORF could potentially improve T cell responses.

Materials and Methods

DNA Constructs and Cell Lines. The complementary DNAs (cDNAs) encoding mouse and human B7.1 (NM_009855.2 and NM_005191.3) and B7.2 (NM_019388.3 and NM_175862.4) and mouse PD-L1 (NM_021893) and PD-L2 (NM_021396) were obtained from C57BL/10 mouse splenocytes and human lymphoblastoid cell line MOU (ECACC 88052050), respectively, by RT-PCR. The cDNAs were subcloned into the pMSCV- or pMXs-based retroviral expression vector as described previously (47). B6/WT3 MEFs (H-2^b) (48) and CHO cells (American Type Culture Collection [ATCC]) were transduced by each of above constructs as described (49). All transduced cells and cell lines CH27 (mouse B cell lymphoma), DC2.4 (mouse DC), RMAS (mouse T cell lymphoma), MRC-5 (human fibroblast), Raji and RPMI8866 (human B lymphoma), Jurkat and CCRF-CEM (human T lymphoblast), and U937 and THP-1 (human monocyte) from the ATCC were maintained in complete RPMI 1640 supplemented with 10% fetal calf serum (HyClone). The constructs expressing the other B7 family members, including pCMV.SPORT6.huB7-H2 (NM_015259.5), pEF6.huB7-H3Δcytoplasmic tail (NM_001024736.1), pCMV3flag-huB7-H4 (NM_024626.3), and pCMV3flag-huB7-H6 (NM_001202439.2), were a gift from Marco Colonna, Washington University in St. Louis.

Protein Production, Purification, and Biotinylation. The sequence encoding M2 (*CPXV040* ORF; Gene ID: 1485915) and C8 [*CPXV028* ORF; a putative PIE protein (4), served as a negative control in this study] were PCR-amplified from CPXV Brighton Red ($CPXV^{BR}$)-infected Vero cells and cloned into the mammalian expression vector pFM1.2 (50) with a 6His tag fused at the C terminus. M2 and control PIE protein were purified from supernatant of pFM1.2-M2–transfected Expi293F cells 72 h posttransfection using nickel agarose beads (Goldbio) followed by size exclusion chromatography on a HiLoaD 26/60 Superdex 200 pg column (GE Healthcare). An aliquot of the purified protein was biotinylated using EZ-Link NHS-PEG_4-Biotin (Thermo Fisher Scientific).

Antibodies and Reagents. Antibodies to human B7.1 (clone L307.4), mouse B7.2 (clone GL1), and mouse B7.1 (clone 16-10A1) and isotype controls were obtained from BD Pharmingen or eBioscience, while anti-human CD86 (clone BU63) and Flag (M2) antibodies were from Serotech and Sigma–Aldrich, respectively. The recombinant mouse and human CD28, CTLA4, and PD-L1, all fused with Fc of human IgG1 at the C terminus (except human PD-L1, fused with Fc of mouse IgG1) were from Sino Biological, Inc. In flow cytometric analysis, stainings of these Fc-fusions were visualized by Alexa Fluor 488- or 647-labeled goat anti-human or mouse IgG (Life Technologies), while biotinylated M2 and controls were detected by PE Streptavidin (BD Pharmingen).

Liquid Chromatography MS/MS Analyses. RPMI8866 cells were lysed in lysing buffer (1% Nonidet P-40 in Tris-buffered saline [TBS] [20 mM Tris·HCl (pH 7.4), 150 mM NaCl] with 20 mM iodoacetamide [IAA] and complete protease inhibitors [Roche]) for 1 h. The lysate was excluded of debris and nuclei by centrifugation at 18,000 × *g* for 15 min and precleared with NeutrAvidin agarose. Precleared lysates, after dilution with TBS/IAA and protease inhibitors to 0.1% Nonidet P-40, were incubated with 100 nM bio-M2 or bio-PIE control and NeutrAvidin agarose for 2 h at 4 °C. The precipitates were eluted with LDS Sample Buffer (Thermo Fisher Scientific) and separated by sodium dodecyl sulfate polyacrylamide gel electrophoresis. The excised gel bands were reduced and alkylated prior to trypsin digestion. Alternatively, the precipitates were eluted with 6 M urea-Tris buffer (50 mM Tris [pH 8.0]), reduced, and alkylated prior to trypsin/Lys-C digestion (Promega) in solution as instructed. The digested peptides in 5% acetonitrile and 1% formic acid were analyzed by liquid chromatography (LC)-MS with Dionex RSLCnano high performance liquid chromatography coupled to a Q Exactive or LTQ-Orbitrap Velos Pro mass spectrometer (Thermo Fisher Scientific). All MS/MS

data were searched against the human database UniProt Knowledgebase (http://www.uniprot.org/) and contaminants using Mascot (Matrix Science). Scaffold_4.8.2 (Proteome Software, Inc.) was used to validate the peptide and protein identification. LC-MS/MS analyses were conducted at the Proteomics & Mass Spectrometry Facility of the Danforth Plant Science Center.

Generation of M2-Deficient CPXV. $CPXV^{BR}$ was kindly provided by Karsten Tischer, Freie Universität Berlin, Berlin, Germany (51). *CPXV040* was deleted using en passant mutagenesis as previously described (52) with the primers 5′-GGGATTAATCTTTGTTGGATCAGTCTCTAAGTTAACACACGTCTTACACAATAG TACGATGCTAGGGATAACAGGGTAATCGATTT-3′ and 5′-TCCATTGTCTTATTGC-TAATTGCATCGTACTATTGTGTAAGACGTGTGTTAACTTAGAGACTGGCCAGTGTT ACAACCAATTAACC-3′. The generated mutant (termed ΔM2 CPXV in this study) was verified by next-generation sequencing.

Ex Vivo T Cell Activation, Proliferation, and IL-2 Assays. Mouse splenic T cells from C57BL/6 mice were enriched by passing through a nylon wool column (53). Enriched T cells were cultured at 2.5 to 5×10^5 cells per well with 0.5 to 1×10^5 cells per well of MEF-mB7.1 or MEF-mB7.2 cells or CH27 cells in a 96-well plate precoated with 50 μL of 0.5 μg/mL hamster anti-mouse CD3ε (clone 500A2; BD Pharmingen). Purified M2 or PIE control, mouse CTLA4-Fc, anti-mouse B7.2 (GL1), or isotype IgG was added in culture at the concentration specified. After incubation at 37 °C for 48 h, IL-2 in culture supernatant was assessed by ELISA in triplicate using an anti-mouse IL-2 antibody pair (JES6-1A12 and JES6-5H4; BioLegend) for capture and detection. For proliferation assays, the enriched splenic T cells were stained with 10 μM CFSE (Life Tech) at 37 °C for 15 min before coculture with the MEF-mB7.2 cells in the presence or absence of indicated antagonists. CFSE dilution in the $CD3^+CD4^+$ population was analyzed 3 d later by flow cytometry. Viral culture supernatants were obtained by infecting Vero cells in a 24-well plate with either WT or ΔM2 CPXV at a MOI 1.0 or 0.5. The culture media were collected at 8, 12, 24, and 48 h postinfection, spun at 13,000 rpm for 2 h, filtered at 0.22 μm, snap-frozen, and stored at −80 °C until used.

Mice. C57BL/6 mice were purchased from Charles River Laboratories. C57BL/6J and B6.129S2-*Cd28*^{tm1Mak}/J mice were purchased from The Jackson Laboratory. Age- and sex-matched mice were infected at 8 to 12 wk of age. Animal studies were approved by the Animal Studies Committee at Washington University in St. Louis.

In Vivo CPXV Infections and Postinfection Analysis. Mice were infected intraperitoneally with 50,000 plaque-forming units of indicated CPXV in 200 μL of phosphate-buffered saline. At 5 d postinfection, spleens were harvested and splenocytes were isolated. B8R-specific $CD8^+$ T cells were assessed ex vivo. CPXV-reactive IFN-γ–producing $CD8^+$ and $CD4^+$ T cells were assessed upon restimulation in vitro as described earlier (42). Briefly, DC2.4 cells were seeded at 2×10^5 cells per well in 12-well plates in RPMI 1640 (Sigma–Aldrich) containing 10% fetal bovine serum and 55 μM 2-mercaptoethanol. To detect CPXV-specific CD8 T cell IFN-γ production, DC2.4 cells were infected for 4 h with Δ12Δ203 CPXV, which ensures presentation of CPXV antigens on MHC-I (6). For CPXV-specific CD4 T cell IFN-γ production, DC2.4 cells were loaded with the indicated peptides (*SI Appendix*, Fig. S6) that share 100% sequence identity with identified VACV epitopes (43, 54) for 2 h at 37 °C. Next, 5×10^6 splenocytes were added, and GolgiPlug (BD Biosciences) was added 1 h later. After an additional 6 h, the incubation was stopped and the splenocytes were stained for flow cytometry. First, viable cells were discriminated using fixable viability dye (Affymetrix). The following antibodies were used for cell surface staining in 2.4g2 supernatant: CD3 (clone 145-2C11; BD Biosciences), CD8a (clone 53-6.7; Affymetrix), CD4 (clone RM4-5; Affymetrix), NK1.1 (clone PK136; Biolegend), and B8R Tetramer (NIH tetramer facility). For intracellular staining, cells were fixed and permeabilized using Cytofix/Cytoperm solution (BD Biosciences) and stained with anti–IFN-γ antibody (Affymetrix). Samples were acquired using a FACSCanto system (BD Biosciences) and analyzed using FlowJo software (Tree Star). Viral loads were determined by quantitative PCR of *CPXV075* as described previously (55).

ACKNOWLEDGMENTS. We thank Marco Colonna (Washington University in St. Louis) for providing cell lines and sharing constructs, and W.M.Y. and D.H.F. laboratory members for helpful discussions. This work was supported by NIH/National Institute of Allergy and Infectious Diseases Cooperative Agreement 5U19AI10994803 and Center for Structural Genomics of Infectious Diseases (CSGID) Contract HHSN272201700060C.

1. Centers for Disease Control and Prevention (CDC), Multistate outbreak of monkeypox–Illinois, Indiana, and Wisconsin, 2003. *MMWR Morb. Mortal. Wkly. Rep.* **52**, 537–540 (2003).
2. P. Fassbender *et al.*, Generalized cowpox virus infection in a patient with HIV, Germany, 2012. *Emerg. Infect. Dis.* **22**, 553–555 (2016).
3. S. Essbauer, M. Pfeffer, H. Meyer, Zoonotic poxviruses. *Vet. Microbiol.* **140**, 229–236 (2010).
4. C. A. Nelson, M. L. Epperson, S. Singh, J. I. Elliott, D. H. Fremont, Structural conservation and functional diversity of the poxvirus immune evasion (PIE) domain superfamily. *Viruses* **7**, 4878–4898 (2015).
5. D. Alzhanova *et al.*, Cowpox virus inhibits the transporter associated with antigen processing to evade T cell recognition. *Cell Host Microbe* **6**, 433–445 (2009).
6. M. Byun *et al.*, Two mechanistically distinct immune evasion proteins of cowpox virus combine to avoid antiviral CD8 T cells. *Cell Host Microbe* **6**, 422–432 (2009).
7. W. H. McCoy, 4th, X. Wang, W. M. Yokoyama, T. H. Hansen, D. H. Fremont, Structural mechanism of ER retrieval of MHC class I by cowpox. *PLoS Biol.* **10**, e1001432 (2012).
8. D. J. Lenschow, T. L. Walunas, J. A. Bluestone, CD28/B7 system of T cell costimulation. *Annu. Rev. Immunol.* **14**, 233–258 (1996).
9. L. Chen, D. B. Flies, Molecular mechanisms of T cell co-stimulation and co-inhibition. *Nat. Rev. Immunol.* **13**, 227–242 (2013).
10. P. S. Linsley *et al.*, CTLA-4 is a second receptor for the B cell activation antigen B7. *J. Exp. Med.* **174**, 561–569 (1991).
11. M. K. Callahan, M. A. Postow, J. D. Wolchok, Targeting T cell co-receptors for cancer therapy. *Immunity* **44**, 1069–1078 (2016).
12. J. H. Esensten, Y. A. Helou, G. Chopra, A. Weiss, J. A. Bluestone, CD28 costimulation: From mechanism to therapy. *Immunity* **44**, 973–988 (2016).
13. E. M. Bertram, W. Dawicki, T. H. Watts, Role of T cell costimulation in anti-viral immunity. *Semin. Immunol.* **16**, 185–196 (2004).
14. S. Ishido *et al.*, Inhibition of natural killer cell-mediated cytotoxicity by Kaposi's sarcoma-associated herpesvirus K5 protein. *Immunity* **13**, 365–374 (2000).
15. L. Coscoy, D. J. Sanchez, D. Ganem, A novel class of herpesvirus-encoded membrane-bound E3 ubiquitin ligases regulates endocytosis of proteins involved in immune recognition. *J. Cell Biol.* **155**, 1265–1273 (2001).
16. A. Loewendorf *et al.*, Identification of a mouse cytomegalovirus gene selectively targeting CD86 expression on antigen-presenting cells. *J. Virol.* **78**, 13062–13071 (2004).
17. J. D. Mintern *et al.*, Viral interference with B7-1 costimulation: A new role for murine cytomegalovirus fc receptor-1. *J. Immunol.* **177**, 8422–8431 (2006).
18. M. Moutaftsi, A. M. Mehl, L. K. Borysiewicz, Z. Tabi, Human cytomegalovirus inhibits maturation and impairs function of monocyte-derived dendritic cells. *Blood* **99**, 2913–2921 (2002).
19. L. Hertel, V. G. Lacaille, H. Strobl, E. D. Mellins, E. S. Mocarski, Susceptibility of immature and mature Langerhans cell-type dendritic cells to infection and immunomodulation by human cytomegalovirus. *J. Virol.* **77**, 7563–7574 (2003).
20. R. Arens *et al.*, B7-mediated costimulation of CD4 T cells constrains cytomegalovirus persistence. *J. Virol.* **85**, 390–396 (2011).
21. M. Fang, L. J. Sigal, Direct CD28 costimulation is required for CD8+ T cell-mediated resistance to an acute viral disease in a natural host. *J. Immunol.* **177**, 8027–8036 (2006).
22. S. Salek-Ardakani *et al.*, Preferential use of B7.2 and not B7.1 in priming of vaccinia virus-specific CD8 T cells. *J. Immunol.* **182**, 2909–2918 (2009).
23. S. J. Goebel *et al.*, The complete DNA sequence of vaccinia virus. *Virology* **179**, 247–266 (1990).
24. A. V. Collins *et al.*, The interaction properties of costimulatory molecules revisited. *Immunity* **17**, 201–210 (2002).
25. M. J. Butte, V. Peña-Cruz, M. J. Kim, G. J. Freeman, A. H. Sharpe, Interaction of human PD-L1 and B7-1. *Mol. Immunol.* **45**, 3567–3572 (2008).
26. M. J. Butte, M. E. Keir, T. B. Phamduy, A. H. Sharpe, G. J. Freeman, Programmed death-1 ligand 1 interacts specifically with the B7-1 costimulatory molecule to inhibit T cell responses. *Immunity* **27**, 111–122 (2007).
27. A. Chaudhri *et al.*, PD-L1 binds to B7-1 only *in cis* on the same cell surface. *Cancer Immunol. Res.* **6**, 921–929 (2018).
28. D. Sugiura *et al.*, Restriction of PD-1 function by *cis*-PD-L1/CD80 interactions is required for optimal T cell responses. *Science* **364**, 558–566 (2019).
29. D. J. Lenschow *et al.*, Differential effects of anti-B7-1 and anti-B7-2 monoclonal antibody treatment on the development of diabetes in the nonobese diabetic mouse. *J. Exp. Med.* **181**, 1145–1155 (1995).
30. D. J. Lenschow *et al.*, Differential up-regulation of the B7-1 and B7-2 costimulatory molecules after Ig receptor engagement by antigen. *J. Immunol.* **153**, 1990–1997 (1994).
31. A. H. Sharpe, G. J. Freeman, The B7-CD28 superfamily. *Nat. Rev. Immunol.* **2**, 116–126 (2002).
32. A. M. Doyle *et al.*, Induction of cytotoxic T lymphocyte antigen 4 (CTLA-4) restricts clonal expansion of helper T cells. *J. Exp. Med.* **194**, 893–902 (2001).
33. M. L. Alegre *et al.*, Regulation of surface and intracellular expression of CTLA4 on mouse T cells. *J. Immunol.* **157**, 4762–4770 (1996).
34. C. C. Stamper *et al.*, Crystal structure of the B7-1/CTLA-4 complex that inhibits human immune responses. *Nature* **410**, 608–611 (2001).
35. X. Zhang, J. C. Schwartz, S. C. Almo, S. G. Nathenson, Crystal structure of the receptor-binding domain of human B7-2: Insights into organization and signaling. *Proc. Natl. Acad. Sci. U.S.A.* **100**, 2586–2591 (2003).
36. S. Ikemizu *et al.*, Structure and dimerization of a soluble form of B7-1. *Immunity* **12**, 51–60 (2000).

37. E. Lazear, L. W. Peterson, C. A. Nelson, D. H. Fremont, Crystal structure of the cowpox virus-encoded NKG2D ligand OMCP. *J. Virol.* **87**, 840–850 (2013).
38. D. M. Harlan, R. Abe, K. P. Lee, C. H. June, Potential roles of the B7 and CD28 receptor families in autoimmunity and immune evasion. *Clin. Immunol. Immunopathol.* **75**, 99–111 (1995).
39. E. A. Tivol, A. N. Schweitzer, A. H. Sharpe, Costimulation and autoimmunity. *Curr. Opin. Immunol.* **8**, 822–830 (1996).
40. J. A. Bluestone, E. W. St Clair, L. A. Turka, CTLA4Ig: Bridging the basic immunology with clinical application. *Immunity* **24**, 233–238 (2006).
41. R. L. Crepeau, M. L. Ford, Challenges and opportunities in targeting the CD28/CTLA-4 pathway in transplantation and autoimmunity. *Expert Opin. Biol. Ther.* **17**, 1001–1012 (2017).
42. M. D. Gainey, J. G. Rivenbark, H. Cho, L. Yang, W. M. Yokoyama, Viral MHC class I inhibition evades CD8+ T-cell effector responses in vivo but not CD8+ T-cell priming. *Proc. Natl. Acad. Sci. U.S.A.* **109**, E3260–E3267 (2012).
43. N. A. Siciliano *et al*., Impact of distinct poxvirus infections on the specificities and functionalities of CD4+ T cell responses. *J. Virol.* **88**, 10078–10091 (2014).
44. B. Moss, Reflections on the early development of poxvirus vectors. *Vaccine* **31**, 4220–4222 (2013).
45. J. Bell, G. McFadden, Viruses for tumor therapy. *Cell Host Microbe* **15**, 260–265 (2014).
46. P. Kleinpeter *et al*., By binding CD80 and CD86, the vaccinia virus M2 protein blocks their interactions with both CD28 and CTLA4 and potentiates CD80 binding to PD-L1. *J. Virol.* **93**, e00207-19 (2019).
47. X. Wang, R. Connors, M. R. Harris, T. H. Hansen, L. Lybarger, Requirements for the selective degradation of endoplasmic reticulum-resident major histocompatibility complex class I proteins by the viral immune evasion molecule mK3. *J. Virol.* **79**, 4099–4108 (2005).
48. J. Pretell, R. S. Greenfield, S. S. Tevethia, Biology of simian virus 40 (SV40) transplantation antigen (TrAg). V in vitro demonstration of SV40 TrAg in SV40 infected nonpermissive mouse cells by the lymphocyte mediated cytotoxicity assay. *Virology* **97**, 32–41 (1979).
49. L. Lybarger, X. Wang, M. R. Harris, H. W. Virgin, 4th, T. H. Hansen, Virus subversion of the MHC class I peptide-loading complex. *Immunity* **18**, 121–130 (2003).
50. F. Mancia *et al*., Optimization of protein production in mammalian cells with a coexpressed fluorescent marker. *Structure* **12**, 1355–1360 (2004).
51. S. J. Roth *et al*., Recovery of infectious virus from full-length cowpox virus (CPXV) DNA cloned as a bacterial artificial chromosome (BAC). *Vet. Res.* **42**, 3 (2011).
52. B. K. Tischer, G. A. Smith, N. Osterrieder, En passant mutagenesis: A two step markerless red recombination system. *Methods Mol. Biol.* **634**, 421–430 (2010).
53. K. S. Hathcock, T cell enrichment by nonadherence to nylon. *Curr. Protoc. Immunol.* Chapter 3:Unit 3.2 (2001).
54. M. Moutaftsi *et al*., Vaccinia virus-specific CD4+ T cell responses target a set of antigens largely distinct from those targeted by CD8+ T cell responses. *J. Immunol.* **178**, 6814–6820 (2007).
55. M. A. Pak-Wittel, L. Yang, D. K. Sojka, J. G. Rivenbark, W. M. Yokoyama, Interferon-γ mediates chemokine-dependent recruitment of natural killer cells during viral infection. *Proc. Natl. Acad. Sci. U.S.A.* **110**, E50–E59 (2013).